

Characterizing larval swordfish habitat in the western tropical North Atlantic

Running title: Characterizing larval swordfish habitat

JUSTIN J. SUCA^{1,2*}, LEIF K. RASMUSON^{1,3,4}, ESTRELLA MALCA^{1,3}, TRIKA GERARD^{3,5},
JOHN T. LAMKIN³

1. *Cooperative Institute of Marine and Atmospheric Studies, University of Miami, 4600 Rickenbacker Causeway, Miami, FL, 33149*

2. *Biology Department, Woods Hole Oceanographic Institution, 266 Woods Hole Rd MS#33, Woods Hole, MA, 02543*

3. *Southeast Fisheries Science Center, NOAA National Marine Fisheries Service, 75 Virginia Beach Drive, Miami, FL 33149, USA*

4. *Marine Resources Program, Oregon Department of Fish and Wildlife, 2040 SE Marine Science Drive, Newport, Oregon 97376, USA*

5. *University of Phoenix, South Florida Campus, 2400 SW 145 Ave, Miramar, FL 33027, USA*

*Email: jsuca@whoi.edu

ABSTRACT:

Swordfish *Xiphias gladius* (Linnaeus, 1758) are a circumglobal pelagic fish targeted by multiple lucrative fisheries. Determining the distribution of swordfish larvae is important for indicating reproductive activity and understanding the early life history of swordfish. We identify and characterize larval swordfish distributions during peak swordfish spawning throughout the Gulf of Mexico and western Caribbean Sea with generalized additive models (GAMs) using catches of swordfish larvae during ichthyoplankton surveys in April and May of 2010, 2011, and 2012. The best fit GAM, as determined by stepwise, backward Akaike Information Criterion selection, included both physiochemical (temperature at 5 m, sea surface height anomaly (SSHA), eddy kinetic energy (EKE)), temporal (lunar illumination, hour of sampling) and spatial (location) variables, while near-surface chlorophyll *a* concentration residuals remained as a random effect. The highest probability of larval swordfish catch occurred at sub-surface temperatures, SSHA, and EKE values indicative of boundary currents. Standard lengths of larvae were larger further downstream in the boundary currents, despite high variability in length with location due to multiple spawning locations of swordfish near these currents. Probability of larval swordfish catch also peaked during the crescent and gibbous moons, indicating a lunar periodicity to swordfish spawning. These results suggest that swordfish may spawn during select moon phases near boundary currents that transport their larvae to larval and juvenile habitat including the northern Gulf of Mexico and coastal waters of the southeast United States.

Key Words: GAM, Larval Habitat, Gulf of Mexico, Caribbean Sea, Xiphiidae, Swordfish

1
2
3
4
5
6
7
8
9
10
11
12
13
14
15
16
17
18
19
20
21
22
23
24
25
26
27
28
29
30
31
32
33
34
35
36
37
38
39
40
41
42
43
44
45
46
47
48
49
50
51
52
53
54
55
56
57
58
59
60

For Peer Review

1 INTRODUCTION:

2 Swordfish *Xiphias gladius* (Linnaeus, 1758) are a circumglobal oceanic fish targeted by
3 multi-million-dollar longline and drift gill net fisheries (Ito *et al.*, 1998; Ward *et al.*, 2000).
4 Swordfish caught in the United States Atlantic Exclusive Economic Zone (EEZ) are primarily
5 members of the Northwest Atlantic stock as defined by the International Commission for the
6 Conservation of Atlantic Tunas (ICCAT, 2014). Swordfish in this stock migrate from the Grand
7 Banks off Newfoundland to the Caribbean Sea and Gulf of Mexico (Palko *et al.*, 1981;
8 Nakamura, 1985; Neilson *et al.*, 2014). Juvenile swordfish (< 130 cm) prefer warmer waters such
9 as the Gulf of Mexico and waters of the southeast US, while larger swordfish primarily occupy
10 waters with colder surface temperatures, such as Georges Bank (Muhling *et al.*, 2015).

11 In addition to large scale geographical migrations, adult swordfish are vertical migrators,
12 spending nights near the surface and diving to depths of ~900 m during daylight (Takahashi *et*
13 *al.*, 2003; Abascal *et al.*, 2010). This behavior matches the similar vertical migration of their prey
14 items: squid and mesopelagic fishes (Scott and Tibbo, 1968; Chancollon *et al.*, 2006). Further,
15 the extent of vertical migration is influenced by the lunar phase with swordfish ascending to
16 shallower (deeper) depths in low (high) lunar illumination (Lerner *et al.*, 2013).

17 Northwest Atlantic swordfish populations spawn year-round in the Atlantic, from Cape
18 Hatteras to the waters North of Puerto Rico (see Fig. 1), including the Caribbean Sea and Gulf of
19 Mexico (Arata, 1954; Grall *et al.*, 1983; Govoni *et al.*, 2000; 2003; Bremer *et al.*, 2005). Most
20 spawning occurs between December and June in the Gulf of Mexico and Caribbean (Taylor and
21 Murphy, 1992; Arocha, 1997; Govoni *et al.*, 2003). The neustonic eggs of swordfish spawned in
22 the Caribbean Sea (where average temperatures are ~25°C) take approximately three days to
23 hatch (Yasuda *et al.*, 1978; Enfield and Mayer, 1997). After hatching, pre-flexion swordfish
24 larvae occupy the upper 10 m of the water column, exclusively consuming copepods (Govoni *et*

1
2
3 25 *al.*, 2003). Swordfish larvae become neustonic and piscivorous at approximately two weeks of
4
5
6 26 age, corresponding to notochord flexion (Govoni *et al.*, 2003).
7

8 27 Swordfish larvae of various sizes have been found throughout the western Atlantic and
9
10 28 Caribbean, resulting in uncertainty in their spawning locations. Grall *et al.* (1983) observed small
11
12 29 larvae (<10 mm) in the eastern Caribbean and Straits of Florida and larger larvae (> 10mm) near
13
14
15 30 the western Antilles. Govoni *et al.*, (2000) suggested that larvae may be spawned as far north as
16
17 31 Cape Hatteras. Further, estimations of spawning locations for swordfish larvae caught in the Gulf
18
19 32 of Mexico and Caribbean have ranged from the north central Gulf of Mexico to the eastern
20
21 33 Caribbean, suggesting spawning may occur as far south as the southern extent of the Sargasso
22
23 34 Sea and the beginning of the Caribbean Current (Govoni *et al.*, 2003). Distribution and larval
24
25 35 habitat have also been described for swordfish larvae in the north central Gulf of Mexico,
26
27 36 suggesting that spawning may occur within the Gulf of Mexico (Rooker *et al.*, 2012). However,
28
29 37 the spatial and temporal extent of many of these studies were limited, with either a limited intra-
30
31 38 seasonal spatial extent or spatially limited to regions in the Gulf of Mexico or southeastern
32
33 39 United States (Govoni *et al.*, 2000; Rooker *et al.*, 2012).
34
35
36
37
38

39 40 Surface transport in the Gulf of Mexico and western Caribbean Sea is dominated by the
40
41 41 Caribbean, Yucatan, and Loop Currents, which become the Florida Current and ultimately the
42
43 42 Gulf Stream after passing through the Straits of Florida (Fig. 1; Oey *et al.*, 2005). The Caribbean
44
45 43 and Loop Currents flow over large zonal distances (≥ 400 km in the case of the Loop Current),
46
47 44 permitting meanders that can separate from the dominant current in the form of mesoscale eddies
48
49 45 (Candela *et al.*, 2002; Richardson, 2005). The Yucatan Current, however, passes through a
50
51 46 topographically constrained channel, resulting in minimal eddy shedding and less variability in
52
53 47 its zonal extent (Oey *et al.*, 2005; Carillo *et al.*, 2016). The fronts associated with boundaries of
54
55
56
57
58
59
60

1
2
3 48 the current systems, as well as the anticyclonic mesoscale eddies they shed, create convergence
4
5 49 zones that concentrate plankton and form essential habitat for pelagic organisms (Bakun, 1996;
6
7
8 50 2006). These convergent zones in the Gulf of Mexico and Caribbean Sea are often used for
9
10 51 spawning and larval habitat by large pelagic fishes such as Atlantic bluefin tuna *Thunnus thynnus*
11
12 52 (Linnaeus, 1758) and sailfish *Istiophorus platypterus* (Shaw, 1792; Teo *et al.*, 2007; Richardson
13
14 53 *et al.*, 2009; Muhling *et al.*, 2010; Simms *et al.*, 2010). Areas of convergence, such as the Gulf
15
16 54 Stream front, serve as habitats for pre-flexion larvae because due to their ability to concentrate
17
18 55 larval swordfish (Govoni *et al.*, 2000). Rooker *et al.*, (2012) also showed that the greatest
19
20 56 probabilities of larval swordfish catches are associated with the Loop Current boundary, further
21
22 57 suggesting that fronts may serve as larval swordfish habitat.
23
24
25
26

27 58 Data from ichthyoplankton surveys along with oceanographic parameters can begin to
28
29 59 elucidate seasonal patterns of larval fish distributions (Houde *et al.*, 1979; Hernandez *et al.*,
30
31 60 2010; Muhling *et al.*, 2010; 2012; Domingues *et al.*, 2016). Habitat models can be formed using
32
33 61 catch data and bio-physical data collected during surveys to predict larval fish distributions to
34
35 62 better understand the diversity and abundance of these larvae in the pelagic environment (Rooker
36
37 63 *et al.*, 2012). The purpose of this work was to identify and predict larval swordfish distributions
38
39 64 during the months of April and May, encompassing part of the peak spawning for swordfish
40
41 65 throughout the Gulf of Mexico and western Caribbean Sea (Govoni *et al.*, 2003). This provides
42
43 66 an opportunity to assess the distribution of swordfish in this region during the same season for
44
45 67 three consecutive years, significantly improving our current understanding of larval swordfish
46
47 68 distribution and swordfish spawning. Based on observations of swordfish larvae in the Gulf of
48
49 69 Mexico and Caribbean, we hypothesized that larvae will most likely to be found in the
50
51 70 Caribbean, Yucatan, and Loop Currents which may serve to transport larvae to suitable habitat to
52
53
54
55
56
57
58
59
60

1
2
3 71 optimize growth and/or survival. This work assesses this hypothesis through formation of habitat
4
5 72 models to improve our understanding of the life history of swordfish and further predicts
6
7
8 73 spawning locations based on the size of larvae collected.
9

10
11 74

12
13 **METHODS:**

14
15 76 Data collected during the 2010-2012 Southeast Area Monitoring and Assessment
16
17 77 Program (SEAMAP) Spring Ichthyoplankton Surveys were used to determine how
18
19
20 78 oceanographic features influence the presence/absence of swordfish larvae. Sampling occurred
21
22 79 during the months of April and May in the western Gulf of Mexico, the edge of the Loop
23
24
25 80 Current, and the Yucatan Channel. Western Caribbean sampling regions varied by year (Fig. 2).
26
27 81 Plankton tows were conducted at each station undulating a 1 x 2m 0.505 mm mesh net fitted with
28
29 82 a flowmeter (2030R, General Oceanics, Inc) between the surface and 10 m depth for 10 minutes
30
31 83 (hereafter referred to as S-10; Habtes *et al.*, 2014). Additional neuston tows were also conducted
32
33
34 84 for 10 min at various stations using a 1 x 2m 0.947 mm mesh net. Tows were conducted during
35
36 85 both day and night. Volume filtered for each tow (m^3) was calculated from flowmeter counts. At
37
38
39 86 most stations a Seabird SBE 9/11 Plus CTD (conductivity, temperature, and depth) equipped
40
41 87 with a dissolved oxygen sensor (SBE 43) was deployed to 300 m. CTD casts were restricted to
42
43
44 88 50 m above the bottom for stations shallower than 350 m.

45
46 *Data Processing/Physical Variables:*

47
48 90 Swordfish larvae were identified using morphological characteristics by the Sea Fisheries
49
50 91 Institute, Plankton Sorting and Identification Center in Szczecin, Poland. Body length was
51
52 92 measured as standard length (SL) or notochord length (NL) to the nearest 0.05 mm (Supp. Table
53
54
55 93 1). Maps of the presence/absence and SL of swordfish larvae for each cruise were generated
56
57
58
59
60

1
2
3 94 using Esri ArcGIS system (Desktop 10.4.1). Sea surface temperature data from the Hybrid
4
5 95 Coordinate Ocean Model (HYCOM) 1/12° resolution Global Reanalysis
6
7
8 96 (<http://hycom.org/data/glb08/expt-19pt1>) were interpolated using the Marine Geospatial
9
10 Ecology Toolbox across the sampling region (Roberts *et al.*, 2010).
11

12
13 98 Physicochemical parameters were obtained from in-situ CTD data, satellite data, and
14
15 99 HYCOM for use in habitat model formation. Values for daily average sea surface height
16
17 100 anomaly and current velocity were obtained for each station using HYCOM estimates. Eddy
18
19
20 101 kinetic energy was calculated from these current velocities using the formula:
21

$$[1] \text{ EKE} = \frac{1}{2}(u^2 + v^2)$$

22 102
23
24 103
25
26
27 104
28
29 105 where EKE represents eddy kinetic energy (m^2s^{-2}), u represents zonal velocity and v represents
30
31 106 the meridional velocity. Near-surface chlorophyll a concentrations for each sampling station
32
33 107 were approximated from the eight-day averaged and 9 km resolution Moderate Resolution
34
35 108 Imaging Spectroradiometer (MODIS), courtesy of the NASA Goddard Space Flight Center,
36
37 109 Ocean Ecology Laboratory, Ocean Biology Processing Group, Greenbelt, MD, USA
38
39 110 (https://oceandata.sci.gsfc.nasa.gov/MODIS-Aqua/Mapped/8Day/9km/chlor_a). Bathymetry
40
41 111 (0.03° resolution) at each station was extracted from the NOAA Center for Environmental
42
43 112 Information bathymetry raster (<http://maps.ngdc.noaa.gov/viewers/wcs-client/>). Fraction of lunar
44
45 113 illumination for each sample day was obtained from the US Navy database
46
47 114 (<http://aa.usno.navy.mil/data/docs/MoonFraction.php>).
48
49
50
51
52

53 115 Physicochemical parameters considered in model development were: temperature ($^\circ\text{C}$) at
54
55 116 5 m, temperature ($^\circ\text{C}$) at 100 m, near-surface chlorophyll a concentration residuals calculated by
56
57
58
59
60

1
2
3 117 removing the temperature trend (mg m^{-3}), dissolved oxygen (5 m) residuals calculated by
4
5 118 removing the temperature trend (mg L^{-1}), salinity (5 m), year, hour of day, latitude, longitude,
6
7
8 119 fraction of lunar illumination, depth (m), eddy kinetic energy ($\text{m}^2 \text{s}^{-2}$), sea surface height
9
10 120 anomaly (m), sea surface height anomaly gradient, and eddy kinetic energy gradient (Table 1).
11
12 121 This suite of variables was chosen because they can be used to differentiate and characterize
13
14 122 oceanographic features in the sampling region. Volume of water filtered (m^3), hereafter volume
15
16 123 filtered by the net was log transformed for each station and included to standardize sampling
17
18 124 effort because of positive skew in the volume filtered values. All *in situ* variables (temperature,
19
20 125 dissolved oxygen, and salinity) were determined as the value closest to the desired depth (5 m or
21
22 126 100 m) from the CTD downcast. Residuals of a linear regression with temperature of both
23
24 127 dissolved oxygen and chlorophyll *a* were used because oxygen and chlorophyll *a* were strongly
25
26 128 collinear with temperature ($r=-0.74$, $p<0.01$; $r=-0.49$, $p<0.01$; Fig. 3). The temperature trend was
27
28 129 removed because it drives patterns of both dissolved oxygen and chlorophyll *a* (Garcia and
29
30 130 Gordon, 1992; Feng *et al.*, 2015). Gradient of sea surface height anomaly and gradient of eddy
31
32 131 kinetic energy were calculated as the gradient between the two nearest HYCOM values ($1/12^\circ$
33
34 132 separation) to each station for the day of sampling.
35
36
37
38
39

40
41 133 Stations lacking CTD casts or containing errors in oxygen values due to sensor
42
43 134 malfunction were removed. In addition, stations sampled in continental shelf waters (<200 m
44
45 135 depth) were removed prior to model formation ($n=117$ stations removed in total). This is due to
46
47 136 high hydrographic variability in coastal waters (thus the poor accuracy of HYCOM in these
48
49 137 regions) and previous studies suggesting that swordfish larvae are rare in depths < 200 m (Grall
50
51 138 *et al.*, 1983; Chassignet *et al.*, 2007).
52
53
54

55 139 *Model Formation:*
56
57
58
59
60

1
2
3 140 The aforementioned variables were used to develop generalized additive models (GAMs)
4
5
6 141 in order to explore the effects of the physical environment on the distribution of swordfish larvae
7
8 142 (Hastie and Tibshirani, 1990). GAMs are statistical models that allow a combination of
9
10 143 physicochemical parameters to interact in a non-linear manner with the response variable and are
11
12 144 non-linear extensions of generalized linear models (Barry and Welsh, 2002). These models
13
14 145 provide a means to discover larval habitats that are difficult to identify through linear models and
15
16 146 simple correlations.

17
18
19
20 147 GAMs for this project were developed using the *mgcv* library in R statistical software
21
22 148 (Version 3.2.3) (Wood, 2008; 2017). We developed presence/absence models rather than
23
24 149 abundance (e.g. catch per unit effort) since abundance data for ichthyoplankton can be difficult
25
26 150 to assess due to the patchy distribution of fish larvae and the coarse spatial scale of sampling.
27
28 151 The response variable for all models was the presence/absence of swordfish in the S-10 tows as
29
30 152 these were conducted at each station and showed a higher frequency of swordfish catch than the
31
32 153 neuston net. All predictor variables were tested for covariance and collinearity using a
33
34 154 correlation matrix followed by plotting and calculating Pearson's product-moment correlation
35
36 155 coefficients (r) for each set of covariates. Correlation of predictor variables to the response
37
38 156 variable were then analyzed through single variable GAMs. The predictor variable showing
39
40 157 largest deviance explained when plotted against the response variable was selected for use in the
41
42 158 model. Models were developed using a binomial distribution with a logit link function. Smooth
43
44 159 functions related the response variable (larval presence/absence) to the model parameters,
45
46 160 permitting non-linear relationships. Each smoothing function was permitted three degrees of
47
48 161 freedom to minimize overfitting with the exception of fraction of lunar illumination, which was
49
50 162 permitted five (Sunbland *et al.*, 2009; Rooker *et al.*, 2012). Five degrees of freedom permits the
51
52
53
54
55
56
57
58
59
60

1
2
3 163 fraction of lunar illumination to incorporate sinusoidal and bimodal responses. Response curves
4
5 164 provided visual representations of the smooth functions to qualitatively relate patterns of
6
7
8 165 presence/absence to physicochemical parameters.

9
10 166 Three parameters were removed due to collinearity: temperature at 100 m (collinear with
11
12 167 temperature at 5m, $r=0.62$), EKE gradient (collinear with temperature at 5m, $r=-0.45$), and sea
13
14 168 surface height anomaly gradient (collinear with EKE, $r=0.55$). After removal of these variables,
15
16 169 the base model included eleven predictor variables and was developed using the following
17
18 170 equation:

19
20
21
22 171 [2] Swordfish presence=offset(log(Volume filtered))+s(Temperature at 5 m)+s(Oxygen
23
24 172 residuals) + s(Chlorophyll-*a* residuals) + s(Salinity at 5 m) + s(Fraction of Lunar Illumination) +
25
26 173 s(Depth) + s(Sea Surface Height) + s(Eddy Kinetic Energy) + te(Longitude, Latitude) + s(Hour of
27
28
29 174 Sampling)+Year

30
31 175 Where s represents a smooth function and te represents a tensor spline, which allows longitude
32
33 176 and latitude to interact anisotropically (Zurr, 2012; Wood, 2017).

34
35
36 177 A stepwise backwards Akaike Information Criterion (AIC) method was used to select the
37
38 178 best fit model. AIC is calculated using the following formula

39
40
41 179
42
43 180 [3] $AIC = -2l + 2k$

44
45 181
46
47
48 182 where l is the maximized log likelihood and K is the number of estimable parameters (Burnham
49
50 183 and Anderson, 2002). The model that resulted in the lowest AIC was selected for each iteration
51
52 184 with the exception of situations where the response curves did not permit reasonable ecological
53
54
55 185 inference. Model selection was further verified by examining the Akaike weights for each
56
57
58
59
60

1
2
3 186 iteration of models to select the best model. Akaike weights are calculated through the following
4
5 187 equation:

6
7
8
9 188
$$[4] w_i = \frac{\exp[-\frac{1}{2}\Delta_i]}{\sum_{i=0}^n \exp[-\frac{1}{2}\Delta_i]}$$

10
11
12 189 Where Δ_i represents the difference in AIC of a particular model from the lowest AIC for any
13
14 190 model in that iteration. Akaike weights can be interpreted as the probability that a model is the
15
16 191 best model for the iteration (Burnham and Anderson, 2002).

17
18
19 192 Once a best-fit model was determined, bootstrapping was used to make a Receiver
20
21 193 Operating Characteristic (ROC) curve and measure the area under that curve (AUC). A randomly
22
23 194 selected subset of 120 stations was used as a training data set (approximately one quarter of the
24
25 195 data) with the remaining data serving as the test data set (Huberty, 1994). The true positive rate
26
27 196 of the bootstrap simulation was plotted against the false positive rate to create a ROC curve. The
28
29 197 integration of this curve results in an AUC value. AUC values close to one represent a good fit of
30
31 198 the model to the data set, with values exceeding 0.90 considered excellent. This bootstrapping
32
33 199 was repeated 1000 times and the mean, median, and standard deviation of these AUC scores
34
35 200 were calculated.

36
37
38 201
39
40
41
42
43 202 **RESULTS:**

44
45 203 One hundred and ninety-seven swordfish larvae were collected from S-10 and neuston
46
47 204 nets over the three years of sampling with 78 of 603 (12.96%) stations sampled positive for
48
49 205 presence of swordfish larvae (Fig. 2). Mapping of swordfish catch with monthly mean sea
50
51 206 surface temperature showed a clear association of swordfish larvae with the waters of Caribbean
52
53 207 Current, Yucatan Current, and Loop Current. The only exceptions were in two stations
54
55
56
57
58
59
60

1
2
3 208 containing swordfish larvae near the continental rise of the northwest Gulf of Mexico in 2012
4
5
6 209 (Fig. 2c)

7
8 210 Larger swordfish larvae (>6.5mm) were also generally caught in the Loop Current with
9
10 211 small individuals (<6.5 mm) being more present near the Yucatan and Caribbean Currents (Fig.
11
12 212 4). The exception was 2012 which showed small larvae near the southeastern extent of the Loop
13
14
15 213 Current as it becomes the Florida Current. There were also three stations containing large
16
17 214 swordfish larvae near Hispaniola in 2011. No significant correlation with latitude and standard
18
19 215 length of swordfish was found ($r=0.05$, $p=0.63$). Smaller individuals were also present in the
20
21 216 northern and western Loop Current in 2010 and 2011 while eastern extent of the Loop Current
22
23 217 primarily contained larger larvae in these years.

24
25
26
27 218 *Model:*

28
29 219 Four hundred and eighty-six stations remained (62 stations containing swordfish larvae)
30
31 220 after oxygen outliers, stations without CTD casts, and shelf waters were removed from the
32
33 221 dataset for model formation (Fig. 2).

34
35
36 222 Seven variables remained in the model after a backwards step-wise AIC model selection:
37
38 223 temperature at 5 m, SSHA, EKE, fraction of lunar illumination, hour of sampling (local time),
39
40 224 and an interaction between latitude and longitude (Table 2). Chlorophyll *a* residuals were also
41
42 225 included as a random effect in the model as they reduced residual heterogeneity (Zurr *et al.*,
43
44 226 2009). This was because the smooth function of chlorophyll *a* residuals was not significant in the
45
46 227 model, but did show collinearity when plotted against residuals of a GAM that did not include
47
48 228 chlorophyll *a* residuals.

49
50
51
52
53 229 The final AIC for this model was 290.542 and the total deviance explained (DE) was
54
55 230 33.1% (Table 3). The variables in order of greatest Δ AIC were longitude and latitude (Δ AIC

1
2
3 231 =19.02, Δ DE=6.3%), percent lunar illumination (Δ AIC =17.91, Δ DE=7.7%), temperature at five
4
5 232 meters (Δ AIC =13.65, Δ DE=9.7%), hour of sampling (Δ AIC =9.58, Δ DE=2.0%), sea surface
6
7 233 height anomaly (Δ AIC =8.10, Δ DE=1.9%) and eddy kinetic energy (Δ AIC =2.98, Δ DE=0.1%).
8
9
10 234 The Akaike weight for the model selected in the final iteration was 0.780, which was strongly
11
12 235 indicative of the best-fit model. The ROC curve for the final model indicated a strong predictive
13
14 236 capability of the model within the dataset. The average AUC for 1000 runs was 0.865, a median
15
16 237 AUC of 0.866, and a standard deviation of 0.047.
17
18
19

20 238 Probability of swordfish presence increased as temperature increased from 24°C to 28°C
21
22 239 with highest catch at surface temperatures of 28°C (Fig. 5a). Probability of larval swordfish
23
24 240 catch reached a maximum around 0.17 m SSHA with a near parabolic curve showing lowest
25
26 241 probability around both low (-0.4 m) and high (0.6 m) SSHA (Fig. 5b). Probability of catch
27
28 242 decreased as eddy kinetic energy increased, though the magnitude of additive effect was minimal
29
30 243 (Fig. 5c). Fraction of lunar illumination displayed an uneven sinusoidal pattern with peak
31
32 244 probability of catch occurring prior to gibbous (0.75 illumination) and crescent (0.25
33
34 245 illumination) moons (Fig. 5d). Lowest probability of catch occurred during the quarter-moons
35
36 246 (0.5 illumination). The response curve for hour of collection was significant, but showed little
37
38 247 overall effect on probability of catch. Highest probability occurred between 1000-1500 local
39
40 248 time (Fig. 5e). No significant relationship or pattern between fraction of lunar illumination and
41
42 249 hour of sampling occurred, indicating that these parameters had independent effects on the catch
43
44 250 of swordfish larvae.
45
46
47
48
49
50
51
52

53 252 **DISCUSSION:**
54
55
56
57
58
59
60

1
2
3 253 This study shows a clear association between the presence of larval swordfish and the
4
5 254 fast-moving currents in the western Caribbean Sea and Gulf of Mexico (Fig. 2). Our habitat
6
7
8 255 models corroborate these findings with the highest probabilities of catching larvae at
9
10 256 physicochemical values indicative of these current systems. Additionally, assessment of the
11
12 257 standard length of larvae by region corroborates findings from previous catches of larval
13
14
15 258 swordfish and mature adults that suggest there are likely multiple spawning locations south of
16
17 259 the Gulf of Mexico near the Caribbean Current and Yucatan Channel, with possible spawning
18
19
20 260 occurring in the northern and western extents of the Loop Current (Govoni *et al.*, 2003; Arocha,
21
22 261 2007; Rooker *et al.*, 2012). These concepts have been documented before but this study expands
23
24 262 our knowledge of the physicochemical parameters that constitute larval habitat throughout both
25
26
27 263 the Gulf of Mexico and Caribbean Sea, differentiates the oceanographic features likely used for
28
29 264 spawning by swordfish, indicates a connection between lunar illumination and swordfish
30
31 265 spawning, and documents new locations and abundances of swordfish larvae throughout the
32
33
34 266 western tropical North Atlantic.

35
36 267 The response curve for temperature at 5 m supports this hypothesis, showing a higher
37
38 268 additive effect with increasing temperature. This result suggests the presence of larvae in warm
39
40 269 waters, a characteristic of the Loop Current (Domingues *et al.*, 2016). These values were
41
42
43 270 consistent with Rooker *et al.*, (2012), which observed peak catch of swordfish larvae at
44
45
46 271 temperatures around 28° C. However, their sampling occurred in the warmer months of June and
47
48 272 July in the north central Gulf of Mexico, likely leading to the negative relationship observed
49
50 273 between surface temperature and larval swordfish catch. The response curve for SSHA shows the
51
52
53 274 highest probability of catch around 0.17 m, the same SSHA referenced as indicating the outer
54
55 275 Loop Current boundary (Fig. 5b). This supports the hypothesis that the Loop Current is used as
56
57
58
59
60

1
2
3 276 larval habitat (Leben and Born, 1993; Berger *et al.*, 1996; Hamilton *et al.*, 2000; Leben *et al.*,
4
5 277 2002). This is inconsistent with the findings of Rooker *et al.*, (2012) which found larval
6
7
8 278 swordfish catch to be highest at negative sea surface height anomalies. However, in 2012 we
9
10 279 observed swordfish larvae in northcentral Gulf of Mexico waters in waters with a negative sea
11
12 280 surface height anomaly, yet near the Loop Current boundary (Fig. 6). Therefore, it is possible
13
14 281 that the increased probability of larval swordfish catch Rooker *et al.*, (2012) observed in the
15
16 282 northern Gulf of Mexico is specific to this smaller region and is not consistent throughout the
17
18 283 larger spatial extent of larval swordfish habitat. Further, Rooker *et al.*, (2012) did show a
19
20 284 negative relationship with distance from the Loop Current, suggesting that the Loop Current was
21
22 285 important larval swordfish habitat, corroborating our findings (2012). Eddy kinetic energy (EKE)
23
24 286 shows highest probability of catch, though minimal, near zero eddy kinetic energy (Fig. 5c). This
25
26 287 would be the case in a water mass that exhibits very little meridional or zonal flow such as
27
28 288 common water or fronts (Ducet and Le Traon, 2001). The fastest moving waters of boundary
29
30 289 currents and eddies display higher EKE values, suggesting these regions may not represent larval
31
32 290 swordfish habitat (Richardson, 2005). However, it is worth noting that the deviance explained by
33
34 291 EKE was low (0.1%) and the significance of this parameter may have changed if we were able to
35
36 292 incorporate more stations into model formation near the Yucatan Channel in 2010 (Table 3; Fig.
37
38 293 2).

39
40
41 294 An overview of our sampling and modeling indicate that swordfish do not rely heavily
42
43 295 on mesoscale eddies for spawning and larval habitat. Instead, swordfish larvae remain near and
44
45 296 within large current systems, a significant development in understanding larval swordfish
46
47 297 ecology. Mesoscale eddies were sampled during our collections and are common hydrographic
48
49 298 features in the Gulf of Mexico and Caribbean Sea (Hurlburt and Thompson, 1982; Vukovich and
50
51
52
53
54
55
56
57
58
59
60

1
2
3 299 Maul, 1985; Carton and Chao, 1999). These eddies are often used for spawning and larval
4
5
6 300 transport of pelagic fishes, such as bluefin tuna and billfishes (Richardson *et al.*, 2009; Govoni *et*
7
8 301 *al.*, 2010; Muhling *et al.*, 2010). Therefore, the use of large currents as opposed to mesoscale
9
10 302 eddies for spawning and larval habitat by swordfish represents a life history strategy unique from
11
12 303 other pelagic predatory fishes. These observed patterns of swordfish spawning near fast-moving
13
14 304 currents are similar to the spawning patterns of swordfish in the Mediterranean, where swordfish
15
16 305 spawn near areas with high current velocity such as the Straits of Messina (Megalofonou *et al.*,
17
18 306 1995; Relini *et al.*, 2003). This suggests that spawning near fast-moving currents is a strategy
19
20 307 that is not unique to the North Atlantic swordfish population.
21
22
23

24 308 The warm temperatures of boundary currents can lead to increased growth rates for fish
25
26 309 larvae, which is advantageous for outgrowing a larval stage with abundant predators (Bailey and
27
28 310 Houde, 1989; Houde, 1989). However, to sustain fast growth rates in warm waters, larvae need
29
30 311 ample prey. Boundaries associated with current systems represent convergence zones that
31
32 312 concentrate fish larvae and zooplankton, the prey of swordfish larvae (Bakun, 2006). Thus,
33
34 313 swordfish larvae may use the boundaries of major currents both for their warm waters and prey
35
36 314 abundance (Fig. 6). Specifically, the Loop Current boundary contains large numbers of *Oithona*
37
38 315 spp. copepods, a known prey item of pre-flexion swordfish larvae (Govoni *et al.*, 2003;
39
40 316 Rathmell, 2007). The presence of neustonic flyingfish (Exocoetidae) and subsurface tuna and
41
42 317 mackerel (Scombridae) larvae may make these boundaries ideal habitat for swordfish larvae as
43
44 318 they transition to piscivory (Arata, 1954; Gorbunova, 1969; Richards *et al.*, 1993; Govoni *et al.*,
45
46 319 2003). However, convergence zones often lead to increased predation pressure and may increase
47
48 320 mortality of swordfish larvae, representing a trade-off between increased food availability and
49
50 321 predation (Bakun, 2006).
51
52
53
54
55
56
57
58
59
60

1
2
3 322 Further, small larvae (< 6 mm SL) were primarily caught north of Honduras, in the
4
5
6 323 Yucatan Channel, and the northern and western extents of the Loop Current, with larger larvae
7
8 324 (> 6 mm SL) occurring on the eastern side of the Loop Current (Fig. 4). However, there was a
9
10 325 great degree of variability in this trend, suggesting that there are multiple spawning locations
11
12 326 throughout the region including the near the Caribbean Current, Yucatan Channel, and the Gulf
13
14 327 of Mexico, corroborating suggestions of these spawning locations from previous studies
15
16 328 (Arocha, 1997; Govoni et al., 2003; Arocha, 2007). The general trend of presence of swordfish
17
18 329 larvae in the fast-moving boundary currents and larger larvae occurring in the eastern extent of
19
20 330 the Loop Current supports the assertion that these boundary currents provide a means to transport
21
22 331 larvae further along the western boundary current system of the Atlantic. Data from the NOAA
23
24 332 Pelagic Observer Program indicate that the northern Gulf of Mexico and coastal Atlantic waters
25
26 333 of the southeastern United States are predominately occupied by juvenile swordfish (80-130 cm;
27
28 334 Muhling *et al.*, 2015). Multiple studies have also indicated that the northern Gulf of Mexico and
29
30 335 the waters off the southeastern United States, particularly the Charleston Bump, represent
31
32 336 juvenile habitat (Cramer, 2001; Govoni *et al.*, 2003). These boundary currents can thus serve a
33
34 337 dual purpose as habitat for swordfish larvae and a mechanism to transport larvae toward their
35
36 338 juvenile habitat.

339 Transport of swordfish larvae to juvenile habitat from spawning in or near fast-moving
340 boundary currents well fits the member vagrant hypothesis as larvae spawned in varying
341 locations throughout the Caribbean, Gulf of Mexico, and Straits of Florida will likely be
342 transported to similar locations to begin the later stages of development (Sinclair, 1988).
343 However, swordfish in the North Atlantic are still genetically identified as one population, thus
344 the boundary currents alone do not represent a complete closure of this population because North

1
2
3 345 Atlantic swordfish also spawn south of the Sargasso Sea which likely transports larvae to
4
5
6 346 additional juvenile habitat in the southeastern Caribbean (Arocha, 1997; Bremer *et al.*, 2005;
7
8 347 Arocha, 2007). Swordfish which spawn near these boundary currents and those that spawn in the
9
10
11 348 Sargasso Sea are considered different spawning groups and mixing among the two spawning
12
13 349 groups may not occur until the fish move farther north to adult foraging grounds (Arocha, 2007).
14

15 350 Furthermore, adult swordfish need to be able to detect these boundary currents while they
16
17 351 are at their day-time depths (up to 900 m) to ensure they remain in proximity to preferred
18
19
20 352 spawning locations. These fish may be able to remain near the western boundary current system
21
22 353 through sensing temperature gradients both near the surface and at depth (Podesta *et al.*, 1993;
23
24 354 Sheinbaum *et al.*, 2002; Carrillo *et al.*, 2016). Therefore, large current regimes, such as the
25
26
27 355 Yucatan Current, may represent as spatially stable and easily identifiable region for swordfish to
28
29 356 spawn. Fecund swordfish and swordfish eggs are often caught near these boundary currents,
30
31
32 357 particularly those of the Yucatan Current, furthering evidence that these boundaries represent
33
34 358 spawning habitat (Arocha, 1997; 2007; Leyva-Cruz *et al.*, 2016). Small swordfish larvae were
35
36 359 caught within the boundary currents in multiple regions and the size of swordfish larvae also
37
38
39 360 tends to increase as they are further downstream in the boundary current systems, supporting the
40
41 361 assertion that these boundary currents are important oceanographic features for swordfish
42
43 362 spawning. While presence of larvae in these boundaries does not directly translate to adult
44
45
46 363 swordfish presence, the presence of swordfish eggs and catches of fecund adult swordfish
47
48 364 suggest these current boundaries are important for both swordfish spawning and larval habitat.
49

50 365 The relationship between catchability of swordfish larvae and fraction of lunar
51
52
53 366 illumination suggest a connection between the lunar phase and time of spawning of swordfish.
54
55 367 Highest catchability of small (65% of larvae <6 mm SL) swordfish larvae occurred during
56
57
58
59
60

1
2
3 368 crescent and gibbous moon phases. The high catches of larvae during crescent and gibbous
4
5 369 moons could be a result of spawning during the quarter moon phases given an estimate of three
6
7 370 days prior to hatching and the subsequent growth rate of swordfish larvae (Yasuda *et al.*, 1978;
8
9 371 Enfield and Mayer, 1997; Govoni *et al.*, 2003). Multiple reports show catch per unit effort
10
11 372 (CPUE) increases for the swordfish fishery around first and third quarter moon phases, possibly
12
13 373 indicative of spawning as CPUE is often highest for fisheries during spawning (dos Santos and
14
15 374 Garcia, 2005; Yukami *et al.*, 2009; Poisson *et al.*, 2010; Erisman *et al.*, 2011). The strong
16
17 375 correlation of night time depth of adult swordfish with lunar illumination supports the hypothesis
18
19 376 that the lunar cycle influences the behavior of swordfish (Dewar *et al.*, 2011; Lerner *et al.*,
20
21 377 2013). While the exact spawning time of swordfish is uncertain, our data reveal the importance
22
23 378 of lunar illumination for the spawning of swordfish for the first time.
24
25
26
27
28

29 379 The peak in larval swordfish catch at noon was consistent with observations from Habtes
30
31 380 *et al.* (2014; Fig. 5e). Diel variability in catch of ichthyoplankton in surface water is often due to
32
33 381 diel vertical migration of ichthyoplankton. However, the diet of swordfish larvae suggests a
34
35 382 shallow water existence as young larvae consume neritic copepods and larger larvae are
36
37 383 piscivorous, suggesting a neustonic lifestyle (Arata, 1954; Gorbunova, 1969; Govoni *et al.*,
38
39 384 2003). Thus, while it is difficult to elucidate a reason for the diel trend in larval swordfish catch,
40
41 385 the literature suggests that large scale vertical migrations are unlikely and our results may be an
42
43 386 artifact of sampling otherwise favorable habitat at these hours.
44
45
46
47

48 387 Mapping and habitat models from this study corroborate previous work indicating that
49
50 388 there are oceanographic features throughout the Gulf of Mexico and western Caribbean Sea that
51
52 389 serve as favorable habitat for swordfish larvae. Future work to better understand the habitat
53
54 390 associations of swordfish larvae should focus on sampling multiple oceanographic features to
55
56
57
58
59
60

1
2
3 391 attain better knowledge of their larval distribution throughout the Caribbean Current, Yucatan
4
5
6 392 Current, and Loop Current. Obtaining finer resolution data on the exact water masses and fronts
7
8 393 utilized by these fish for spawning and larval habitat can be used to protect regions from fishing
9
10 394 pressure and shipping disturbance to assist the reproductive success of these fish. However,
11
12 395 intra-annual variability of swordfish spawning needs to be assessed, thus sampling should occur
13
14 396 January through July with a focus on both eggs and larvae in order to elucidate this variation
15
16 397 (Govoni *et al.*, 2003; Rooker *et al.*, 2012; Neilson *et al.*, 2014). Habitat models may also be
17
18 398 constructed through different methodologies to incorporate historical data from SEAMAP and
19
20 399 Marine Resources Monitoring, Assessment, and Prediction program (MARMAP) data sets but
21
22 400 these must be done carefully to ensure the physical parameters are accurate and precise. The
23
24 401 years of sampling in this study (2010-2012) also occurred at a time of low abundance in the
25
26 402 North Atlantic swordfish stock, though recovery of the stock was likely occurring (ICCAT,
27
28 403 2014). Future studies should assess how and if habitat models of larvae may change as the stock
29
30 404 size fluctuates and if the quantity of favorable habitat as predicted by these models relates to
31
32 405 recruitment of this stock.
33
34
35
36
37
38

39 406 We present new developments in the understanding of the early life history of swordfish.
40
41 407 This study supports and expands the spatial extent of the existing hypothesis that larval
42
43 408 swordfish habitat is associated with boundary currents in the western Caribbean Sea and Gulf of
44
45 409 Mexico, primarily the Caribbean, Yucatan, and Loop Currents and that these currents may
46
47 410 provide a means to transport swordfish larvae toward larval and juvenile habitats. Assessment of
48
49 411 the standard length of larvae caught throughout the sampling region indicated that multiple
50
51 412 spawning locations likely occur, with small larvae caught north of Honduras, the Yucatan
52
53 413 Channel, and in the north central Gulf of Mexico in northern and western extents of the Loop
54
55
56
57
58
59
60

1
2
3 414 current. We also indicate a connection between lunar illumination and swordfish spawning, the
4
5
6 415 first assertion of such a connection to our knowledge. While higher resolution data should be
7
8 416 used to further identify smaller scale associations of swordfish larvae with oceanographic
9
10 417 features, the identification of larval habitat from this study is a step toward an improved
11
12 418 understanding of this commercially and ecologically important species. This study provides
13
14
15 419 valuable information about the larval habitat of a commercially important species so that
16
17 420 estimations of anthropogenic influences on larval habitat can be made, including severely
18
19 421 deleterious events such as oil spills.
20
21
22 422
23

24 423 **ACKNOWLEDGMENTS:**

25
26
27 424 The authors would like to thank the lab at the NOAA Fisheries Oceanography for
28
29 425 Recruitment, Climate and Ecosystem Studies (FORCES), the taxonomists at the Departamento
30
31 426 de Sistemática y Ecología Acuática at El Colegio de la Frontera Sur (ECOSUR), the staff at the
32
33 427 Polish Plankton Sorting and Identification Center in Szczecin, Poland, and the officers and crew
34
35 428 of the NOAA ship Gordon Gunter that facilitated data collection on the SEAMAP cruises. The
36
37 429 authors would also like to thank J Serafy for useful comments to improve this manuscript. This
38
39 430 research was carried out under the auspices of the Cooperative Institute for Marine and
40
41 431 Atmospheric Studies, University of Miami and partially funded by NASA (NNX11AP76G,
42
43 432 NNX08AL06G), and the NOAA Southeast Fisheries Science Center. No authors have any
44
45
46 433 conflicts of interest to declare.
47
48
49
50
51 434
52
53
54
55
56
57
58
59
60

REFERENCES:

- Arata Jr, G. F. (1954). A contribution to the life history of the swordfish, *Xiphias gladius* Linnaeus, from the South Atlantic coast of the United States and the Gulf of Mexico. *Bulletin of Maine Science* 4, 183-243.
- Arocha, F. (1997). The reproductive dynamics of swordfish *Xiphias gladius* L and management implications in the northwestern Atlantic. PhD thesis, University of Miami
- Arocha, F. (2007). Swordfish reproduction in the Atlantic Ocean: an overview. *Gulf and Caribbean Research*, 19, 21-36.
- Bakun, A. (1996). *Patterns in the ocean*. La Paz, Mexico: California Sea Grant, in cooperation with Centro de Investigaciones Biologicas del Noroeste
- Bakun, A. (2006). Fronts and eddies as key structures in the habitat of marine fish larvae: opportunity, adaptive response and competitive advantage. *Scientia Marina*, 70, 105-122.
- Bailey, K. M., & Houde, E. D. (1989). Predation on eggs and larvae of marine fishes and the recruitment problem. *Advances in Marine Biology*, 25, 1-83.
- Barry, S. C., & Welsh, A. H. (2002). Generalized additive modelling and zero inflated count data. *Ecological Modelling* 157, 179-188.
- Berger, T. J., P. Hamilton, J. J. Singer, R. R. Leben, G. H. Born & C. A. Fox (1996), Louisiana/Texas Shelf Physical Oceanography Program Eddy Circulation Study: Final Synthesis Report. Volume I: Technical Report, OCS Study MMS 96-0051, U.S. Dept. of the Interior, Minerals Management Service, Gulf of Mexico OCS Region, New Orleans, LA. 324 pp.
- Bremer, J. A., Mejuto, J., Gómez-Márquez, J., Boán, F., Carpintero, P., Rodríguez, J. M., Viñas, J., Greig, T.W., & Ely, B. (2005). Hierarchical analyses of genetic variation of samples from breeding and feeding grounds confirm the genetic partitioning of northwest Atlantic and South Atlantic populations of swordfish (*Xiphias gladius* L.). *Journal of Experimental Marine Biology and Ecology*, 327, 167-182.
- Burnham, K. P., & Anderson, D. R. (2002). Akaike Weights. In *Model Selection and Multimodel Inference: A Practical Information-Theoretic Approach Second Edition* (pp. 60-65). Springer: New York.
- Candela, J., Sheinbaum, J., Ochoa, J., Badan, A., & Leben, R. (2002). The potential vorticity flux through the Yucatan Channel and the Loop Current in the Gulf of Mexico. *Geophysical Research Letters*, 29(22).
- Carrillo, L., Johns, E. M., Smith, R. H., Lamkin, J. T., & Largier, J. L. (2016). Pathways and hydrography in the Mesoamerican Barrier Reef System Part 2: Water masses and thermohaline structure. *Continental Shelf Research*, 120, 41-58.
- Carton, J. A., & Chao, Y. (1999). Caribbean Sea eddies inferred from TOPEX/Poseidon altimetry and a 1/6 Atlantic Ocean model simulation. *Journal of Geophysical Research*, 104(C4), 7743-7752.

- 1
2
3 Chancollon, O., Pusineri, C., & Ridoux, V. (2006). Food and feeding ecology of Northeast
4 Atlantic swordfish (*Xiphias gladius*) off the Bay of Biscay. *ICES Journal of Marine Science:*
5 *Journal du Conseil*, 63, 1075-1085.
6
7
8 Chassignet, E. P., Hurlburt, H. E., Smedstad, O. M., Halliwell, G. R., Hogan, P. J., Wallcraft, A.
9 J., Baraille, R., & Bleck, R. (2007). The HYCOM (hybrid coordinate ocean model) data
10 assimilative system. *Journal of Marine Systems*, 65, 60-83.
11
12 Cramer, J. (2001). Geographic distribution of longline effort and swordfish discard rates in the
13 straits of Florida and oceanic waters of the continental shelf, slope, and Blake Plateau off
14 Georgia and the Carolinas from 1991 to 1995. In *American Fisheries Society Symposium*, 97-104
15
16 Cushing, D. H. (1969). The regularity of the spawning season of some fishes. *ICES Journal of*
17 *Marine Science: Journal du Conseil*, 33, 81-92.
18
19 Cushing, D. H. (1990). Plankton production and year-class strength in fish populations: an
20 update of the match/mismatch hypothesis. *Advances in Marine Biology*, 26, 249-293.
21
22 Dewar, H., Prince, E. D., Musyl, M. K., Brill, R. W., Sepulveda, C., Luo, J., Foley, D., Orbesen,
23 E.S., Dromeier, M.L., Nasby-Lucas, N., Snodgrass, D., Luars, R.M., Hoolihan, J.P. Block, B.A.,
24 & McNaughton, L.M. (2011). Movements and behaviors of swordfish in the Atlantic and Pacific
25 Oceans examined using pop-up satellite archival tags. *Fisheries Oceanography* 20, 219-241.
26
27 Domingues, R., Goni, G., Bringas, F., Muhling, B., Lindo-Atichati, D., & Walter, J. (2016).
28 Variability of preferred environmental conditions for Atlantic bluefin tuna (*Thunnus thynnus*)
29 larvae in the Gulf of Mexico during 1993–2011. *Fisheries Oceanography*, 25, 320-336.
30
31 Ducet, N., & Le Traon, P. Y. (2001). A comparison of surface eddy kinetic energy and Reynolds
32 stresses in the Gulf Stream and the Kuroshio Current systems from merged TOPEX/Poseidon
33 and ERS-1/2 altimetric data. *Journal of Geophysical Research-Oceans*, 106, 16603-16622.
34
35 Enfield, D. B., & Mayer, D. A. (1997). Tropical Atlantic sea surface temperature variability and
36 its relation to El Niño–Southern Oscillation. *Journal of Geophysical Research-Oceans* 102, 929-
37 945.
38
39 Erisman, B. E., Allen, L. G., Claisse, J. T., Pondella, D. J., Miller, E. F., & Murray, J. H. (2011).
40 The illusion of plenty: hyperstability masks collapses in two recreational fisheries that target fish
41 spawning aggregations. *Canadian Journal of Fisheries and Aquatic Sciences*, 68, 1705-1716.
42
43 Feng, J., Durant, J. M., Stige, L. C., Hessen, D. O., Hjermann, D. Ø., Zhu, L., Llope, M., &
44 Stenseth, N.C. (2015). Contrasting correlation patterns between environmental factors and
45 chlorophyll levels in the global ocean. *Global Biogeochemical Cycles* 29, 2095-2107
46
47 Garcia, H. E., & Gordon, L. I. (1992). Oxygen solubility in seawater: Better fitting
48 equations. *Limnology and Oceanography*, 37, 1307-1312.
49
50 Gorbunova, N. N. (1969). Breeding grounds and food of the larvae of the swordfish [*Xiphias*
51 *gladius* Linné (Pisces, Xiphilidae)]. *Problems in Ichthyology*, 9, 375-387.
52
53 Govoni, J. J., Stender, B. W., & Pashuk, O. (2000). Distribution of larval swordfish, *Xiphias*
54 *gladius*, and probable spawning off the southeastern United States. *Fishery Bulletin*, 98, 64-74
55
56
57
58
59
60

- 1
2
3 Govoni, J. J., Laban, E. H., & Hare, J. A. (2003). The early life history of swordfish (*Xiphias*
4 *gladius*) in the western North Atlantic. *Fishery Bulletin*, 101, 778-789.
- 5
6 Govoni, J. J., Hare, J. A., Davenport, E. D., Chen, M. H., & Marancik, K. E. (2010). Mesoscale,
7 cyclonic eddies as larval fish habitat along the southeast United States shelf: a Lagrangian
8 description of the zooplankton community. *ICES Journal of Marine Science: Journal du Conseil*.
9 67, 403-411.
- 10
11 Grall, C., De Sylva, D. P., & Houde, E. D. (1983). Distribution, relative abundance, and
12 seasonality of swordfish larvae. *Transactions of American Fisheries Society*, 112, 235-246.
- 13
14 Habtes, S., Muller-Karger, F. E., Roffer, M. A., Lamkin, J. T., & Muhling, B. A. (2014). A
15 comparison of sampling methods for larvae of medium and large epipelagic fish species during
16 spring SEAMAP ichthyoplankton surveys in the Gulf of Mexico. *Limnology and Oceanography:*
17 *Methods*, 12, 86-101.
- 18
19 Hamilton, P., Berger, T.J., Singer, J.J., Waddell, E., Churchill, J.H., Leben, R.R., Lee, T.N., &
20 Sturges, W., (2000). DeSoto Canyon Eddy Intrusion Study, Final Report, Volume II: Technical
21 Report, OSC Study MMS 2000-080. US Department of the Interior, Minerals Management
22 Service, Gulf of Mexico OCS Region, New Orleans, LA, 275pp.
- 23
24 Hernandez Jr, F. J., Powers, S. P., & Graham, W. M. (2010). Seasonal variability in
25 ichthyoplankton abundance and assemblage composition in the northern Gulf of Mexico off
26 Alabama. *Fishery Bulletin*, 108(2), 193-207.
- 27
28 Houde, E. D., Dowd, J. C., Berkeley, C. E., Houde, S. A. E. D., & James,
29 C.(1979). *Ichthyoplankton abundance and diversity in the eastern Gulf of Mexico* (No. 574.92
30 I2).
- 31
32 Houde, E. D. (1989). Comparative growth, mortality, and energetics of marine fish larvae:
33 temperature and implied latitudinal effects. *Fishery Bulletin*, 87, 471-495.
- 34
35 Huberty, C. J. (1994). *Applied discriminant analysis* (Vol. 297). Wiley-Interscience.
- 36
37 Hurlburt, H. E., & Thompson, J.D. (1982). The dynamics of the loop current and shed eddies in a
38 numerical model of the Gulf of Mexico. In: *Hydrodynamics of Semi-enclosed Seas*, ed. J. C. J.
39 *Nihoul*, Elsevier Science, New York, NY., 243–297
- 40
41 International Commission for the Conservation of Atlantic Tunas (2014). Report of the ICCAT
42 swordfish stock assessment session.
- 43
44 Ito, R. Y., Dollar, R. A., & Kawamoto, K. E. (1998). The Hawaii-based longline fishery for
45 swordfish, *Xiphias gladius*. *Biology and fisheries of swordfish, Xiphias gladius*. NOAA Tech Rep
46 NMFS, 142, 77-88.
- 47
48 Leben, R. R., & Born, G. H. (1993). Tracking Loop Current eddies with satellite
49 altimetry. *Advances in Space Research*, 13, 325-333.
- 50
51 Leben, R. R., Born, G. H., & Engebret, B. R. (2002). Operational altimeter data processing for
52 mesoscale monitoring. *Marine Geodesy*, 25, 3-18.
- 53
54
55
56
57
58
59
60

- 1
2
3 Lerner, J. D., Kerstetter, D. W., Prince, E. D., Talaue-McManus, L., Orbesen, E. S., Mariano, A.,
4 Snodgrass, D., & Thomas, G. L. (2013). Swordfish vertical distribution and habitat use in
5 relation to diel and lunar cycles in the western North Atlantic. *Transactions of the American*
6 *Fisheries Society*, 142, 95-104.
7
8
9 Leyva-Cruz, E., Vásquez-Yeomans, L., Carrillo, L., & Valdez-Moreno, M. (2016). Identifying
10 pelagic fish eggs in the southeast Yucatan Peninsula using DNA barcodes. *Genome*, 59, 1117-
11 1129.
12
13 Megalofonou, P., Dean, J. M., De Metrio, G., Wilson, C., & Berkeley, S. (1995). Age and
14 growth of juvenile swordfish, *Xiphias gladius* Linnaeus, from the Mediterranean Sea. *Journal of*
15 *Experimental Marine Biology and Ecology*, 188(1), 79-88.
16
17 Muhling, B. A., Lamkin, J. T., & Roffer, M. A. (2010). Predicting the occurrence of Atlantic
18 bluefin tuna (*Thunnus thynnus*) larvae in the northern Gulf of Mexico: building a classification
19 model from archival data. *Fisheries Oceanography*, 19, 526-539.
20
21 Muhling, B. A., Lamkin, J. T., & Richards, W. J. (2012). Decadal-scale responses of larval fish
22 assemblages to multiple ecosystem processes in the northern Gulf of Mexico. *Marine Ecology*
23 *Progress Series*, 450, 37-53.
24
25 Muhling, B. A., Liu, Y., Lee, S. K., Lamkin, J. T., Malca, E., Llopiz, J.K., Ingram G. W.,
26 Quattro J. M., Walter, J. F., Doering, K., Roffer, M. A., & Muller-Karger, F. (2015). Past,
27 Ongoing and Future Research on Climate Change Impacts on Tuna and Billfishes in the Western
28 Atlantic. *Collect. Vol. Sci. Pap. ICCAT*, 71, 147-174.
29
30 Nakamura, I. (1985) Billfishes of the world. FAO Fish. Synop. 125, 58 p
31
32 NASA Goddard Space Flight Center, Ocean Ecology Laboratory, Ocean Biology Processing
33 Group. Moderate-resolution Imaging Spectroradiometer (MODIS) Aqua Chlorophyll Data; 2014
34 Reprocessing. NASA OB.DAAC, Greenbelt, MD, USA. doi:
35 10.5067/AQUA/MODIS/L3M/CHL/2014. Accessed on 03/2016
36
37 Neilson, J. D., Loefer, J., Prince, E. D., Royer, F., Calmettes, B., Gaspar, P., Lopez, R., &
38 Andrushchenko, I. (2014). Seasonal Distributions and Migrations of Northwest Atlantic
39 Swordfish: Inferences from Integration of Pop-Up Satellite Archival Tagging Studies. *PLoS*
40 *one*, 9, e112736.
41
42 Oey, L. Y., Ezer, T., & Lee, H. C. (2005). Loop Current, rings and related circulation in the Gulf
43 of Mexico: A review of numerical models and future challenges. *Circulation in the Gulf of*
44 *Mexico: Observations and models*, Washington D.C: AGU
45
46 Palko, R. J., G. L. Beardsley, & W. J. Richards. (1981) Synopsis of the biology of the swordfish
47 *Xiphias gladius* Linnaeus. U.S. Dep. Commer. NOAA Tech. Rep. NMFS Circ. 441.
48
49 Podestá, G. P., Browder, J. A., & Hoey, J. J. (1993). Exploring the association between
50 swordfish catch rates and thermal fronts on US longline grounds in the western North
51 Atlantic. *Continental Shelf Research* 13, 253-277.
52
53
54
55
56
57
58
59
60

- 1
2
3 Poisson, F., Gaertner, J. C., Taquet, M., Durbec, J. P., and Bigelow, K. (2010). Effects of lunar
4 cycle and fishing operations on longline-caught pelagic fish: fishing performance, capture time,
5 and survival of fish. *Fishery Bulletin* 108, 268-281.
- 7 Rathmell, K. (2007). The influence of the Loop Current on the diversity, abundance, and
8 distribution of zooplankton in the Gulf of Mexico. Master's thesis, University of South Florida.
- 10 Relini, L. O., Palandri, G., & Garibaldi, F. (2003). Reproductive parameters of the
11 Mediterranean swordfish. *Bioiogia . Marina Mediterranea*, 10(2), 210-222.
- 13 Richards, W. J., McGowan, M. F., Leming, T., Lamkin, J. T., & Kelley, S. (1993). Larval fish
14 assemblages at the Loop Current boundary in the Gulf of Mexico. *Bulletin of Marine*
15 *Science*, 53, 475-537.
- 17 Richardson, P. L. (2005). Caribbean Current and eddies as observed by surface drifters. *Deep-*
18 *Sea Research Pt. II*, 52, 429-463.
- 20 Richardson, D. E., Llopiz, J. K., Leaman, K. D., Vertes, P. S., Muller-Karger, F. E., & Cowen,
21 R. K. (2009). Sailfish (*Istiophorus platypterus*) spawning and larval environment in a Florida
22 Current frontal eddy. *Progress in Oceanography*, 82, 252-264.
- 24 Richardson, D. E., Llopiz, J. K., Guigand, C. M., & Cowen, R. K. (2010). Larval assemblages of
25 large and medium-sized pelagic species in the Straits of Florida. *Progress in Oceanography*, 86,
26 8-20.
- 28 Roberts, J. J., Best, B. D., Dunn, D. C., Treml, E. A., & Halpin, P. N. (2010). Marine Geospatial
29 Ecology Tools: An integrated framework for ecological geoprocessing with ArcGIS, Python, R,
30 MATLAB, and C++. *Environmental Modelling & Software*, 25, 1197-1207.
- 32 Rooker, J. R., Simms, J. R., Wells, R. D., Holt, S. A., Holt, G. J., Graves, J. E., & Furey, N. B.
33 (2012). Distribution and habitat associations of billfish and swordfish larvae across mesoscale
34 features in the Gulf of Mexico. *PloS one*, 7, e34180.
- 36 dos Santos, M. N., & Garcia, A. (2005). The influence of the moon phase on the CPUEs for the
37 Portuguese swordfish (*Xiphias gladius* L., 1758) fishery. *Col. Vol. Sci. Pap. ICCAT*, 58, 1466-
38 1469.
- 40 Scott, W. B., & Tibbo, S. N. (1968). Food and feeding habits of swordfish, *Xiphias gladius*, in
41 the western North Atlantic. *Journal of the Fisheries Board of Canada*, 25, 903-919.
- 43 Sheinbaum, J., Candela, J., Badan, A., & Ochoa, J. (2002). Flow structure and transport in the
44 Yucatan Channel. *Geophysical Research Letters* 29, 101-104
- 46 Simms, J. R., Rooker, J. R., Holt, S. A., Holt, G. J., & Bangma, J. (2010). Distribution, growth,
47 and mortality of sailfish (*Istiophorus platypterus*) larvae in the northern Gulf of Mexico. *Fishery*
48 *Bulletin*, 108, 478-490.
- 50 Sinclair, M. (1988). *Marine populations: an essay on population regulation and speciation*.
51 Washington Press.
- 52
53
54
55
56
57
58
59
60

- 1
2
3 Solanki, H. U., Bhatpuria, D., & Chauhan, P. (2015). Integrative Analysis of AltiKa-SSHa,
4 MODIS-SST, and OCM-Chlorophyll Signatures for Fisheries Applications. *Marine Geodesy*,
5 38, 672-683.
6
7 Sundblad, G., Härmä, M., Lappalainen, A., Urho, L., & Bergström, U. (2009). Transferability of
8 predictive fish distribution models in two coastal systems. *Estuarine, Coastal and Shelf*
9 *Science*, 83, 90-96.
10
11 Taylor, R. G., & Murphy, M. D. (1992). Reproductive biology of the swordfish *Xiphias gladius*
12 in the Straits of Florida and adjacent waters. *Fishery Bulletin*, 90, 809-816.
13
14 Teo, S. L., Boustany, A. M., & Block, B. A. (2007). Oceanographic preferences of Atlantic
15 bluefin tuna, *Thunnus thynnus*, on their Gulf of Mexico breeding grounds. *Marine Geodesy*, 152,
16 1105-1119.
17
18 Vukovich, F. M., & Maul, G. A. (1985). Cyclonic eddies in the eastern Gulf of Mexico. *Journal*
19 *of Physical Oceanography*, 15, 105-117.
20
21 Ward, P., Porter, J. M., & Elscot, S. (2000). Broadbill swordfish: status of established fisheries
22 and lessons for developing fisheries. *Fish and Fisheries*, 1, 317-336.
23
24 Wood, S. N. (2008). Fast stable direct fitting and smoothness selection for generalized additive
25 models. *Journal of the Royal Statistical Society Series B Statistical Methodology* 70, 495-518.
26
27 Wood, S.N. (2017). *Generalized additive models: an introduction with R*. CRC press.
28
29 Yasuda F, Kohno H, Yatsu A, Ida H, Arena P, Li Greci F, Taki Y (1978) Embryonic and early
30 larval stages of the swordfish, *Xiphias gladius*, from the Mediterranean. *Journal of the Tokyo*
31 *University of Fisheries*, 65, 91-97
32
33 Yukami, R., Ohshimo, S., Yoda, M., & Hiyama, Y. (2009). Estimation of the spawning grounds
34 of chub mackerel *Scomber japonicus* and spotted mackerel *Scomber australasicus* in the East
35 China Sea based on catch statistics and biometric data. *Fisheries Science*, 75, 167-174.
36
37 Zuur, A. F., Ieno, E. N., Walker, N. J., Saveliev, A. A., & Smith, G. M. (2009). Zero-truncated
38 and zero-inflated models for count data. In *Mixed effects models and extensions in ecology with*
39 *R* (pp. 261-293). New York: Springer
40
41 Zuur, A.F. (2012) *A beginner's guide to generalized additive models with R*. Newburgh:
42 Highland Statistics Limited.
43
44
45
46
47
48
49
50
51
52
53
54
55
56
57
58
59
60

1
2
3
4
5
6
7
8
9

TABLES:

Table 1: Environmental parameters used in model formation with sources and metrics listed. All *in-situ* data were collected using a Seabird SBE 9/11 Plus CTD (conductivity, temperature, and depth) equipped with a dissolved oxygen sensor (SBE 43).

10
11
12
13
14
15
16
17
18
19
20
21
22
23
24
25
26
27
28
29
30
31
32
33
34
35
36
37
38
39
40
41
42
43
44
45
46
47
48
49
50
51
52
53
54
55
56
57
58
59
60

Parameter	Source	Minimum	Maximum	Mean	Median
Eddy Kinetic Energy ($\text{m}^2 \text{s}^{-2}$)	HYCOM	0.00	1.54	0.14	0.06
Sea Surface Height Anomaly (m)	HYCOM	-0.45	0.64	-0.09	-0.19
Temperature at 5 m ($^{\circ}\text{C}$)	<i>In-situ</i>	21.45	28.35	26.39	26.66
Salinity at 5 m	<i>In-situ</i>	33.04	36.70	36.04	36.02
Oxygen at 5 m (mg L^{-1})	<i>In-situ</i>	6.13	7.46	6.60	6.61
Chlorophyll <i>a</i> (mg m^{-3})	MODIS	0.04	0.57	0.11	0.10
Depth (m)	NCEI	204.00	7124.00	2177.24	2140.50

1
2
3 **Table 2:** Details of the backward stepwise Akaike Information Criterion (Δ AIC) model selection process
4 including the original model and the subsequent top three models for each iteration as determined by greatest
5 change in AIC and deviance explained. The overall best fit model for the final iteration is in bold. ORT
6 represents oxygen residuals from temperature. CRT (RE) represents chlorophyll *a* residuals from temperature as
7 a random effect.
8
9
10
11
12
13
14
15
16
17
18
19
20
21
22
23
24
25
26
27
28
29
30
31
32
33
34
35
36
37
38
39
40
41
42
43
44
45
46
47
48
49
50
51
52
53
54
55
56
57
58
59
60

For Peer Review

Iteration	Variables Included	AIC (Δ)	DE (Δ)	Akaike Weight(w_i)
1	Temperature, ORT, CRT (RE), SSHA, EKE, Lun Illum, Salinity, Hour, Depth, Year, Long/Lat(TE)	296.33 (0)	33.6(0)	0.126
1	Temperature, ORT, CRT (RE), SSHA, EKE, Lun Illum, Salinity, Hour, Depth, Long/Lat(TE)	295.04(-1.29)	33.1(-0.5)	0.228
1	Temperature, CRT (RE), SSHA, EKE, Lun Illum, Salinity, Hour, Depth, Year, Long/Lat(TE)	294.61(-1.72)	33.2(-0.3)	0.282
1	Temperature, ORT, CRT (RE), SSHA, EKE, Lun Illum, Hour, Depth, Year, Long/Lat(TE)	294.53(-1.80)	33.5(-0.1)	0.294
2	Temperature, ORT, CRT (RE), SSHA, EKE, Lun Illum, Hour, Depth Year, Long/Lat(TE)	294.53(-1.80)	33.5(-0.1)	0.173
2	Temperature, ORT, CRT (RE), SSHA, EKE, Lun Illum, Salinity, Hour, Year, Long/Lat(TE)	296.54(0.210)	30.5(-3.1)	0.063
2	Temperature, ORT, CRT (RE), SSHA, EKE, Lun Illum, Hour, Depth, Long/Lat(TE)	293.43(-2.89)	33(-0.6)	0.299
2	Temperature, CRT (RE), SSHA, EKE, Lun Illum, Hour, Depth, Year, Long/Lat(TE)	292.74(-3.58)	33.2(-0.3)	0.423
3	Temperature, CRT (RE), SSHA, EKE, Lun Illum, Hour, Depth, Year, Long/Lat(TE)	292.74(-3.58)	33.2(-0.3)	0.217
3	Temperature, CRT (RE), SSHA, Lun Illum, Hour, Depth, Year, Long/Lat(TE)	296.66(0.330)	29.4(-4.2)	0.008
3	Temperature, CRT (RE) SSHA, EKE, Lun Illum, Salinity, Hour, Depth, Long/Lat(TE)	292.1(-4.22)	33.1(-0.5)	0.298
3	Temperature, CRT (RE), SSHA, EKE, Lun Illum, Hour, Year, Long/Lat(TE)	291.31(-5.01)	33.1(-0.5)	0.443
4	Temperature, CRT (RE), SSHA, EKE, Lun Illum,, Hour, Year, Long/Lat(TE)	291.31(-5.01)	33.1(-0.5)	0.380
4	Temperature, CRT (RE), EKE, Lun Illum, Hour, Year, Long/Lat(TE)	298(1.670)	30(-3.6)	0.013
4	Temperature, CRT (RE), SSHA, Lun Illum, Hour, Year, Long/Lat(TE)	295.93(-0.39)	29.4(-4.2)	0.038
4	Temperature, CRT (RE), SSHA, EKE, Lun Illum, Hour, Long/Lat(TE)	290.54(-5.78)	33.1(-0.5)	0.558
5	Temperature, CRT (RE), SSHA, EKE, Lun Illum, Hour, Long/Lat(TE)	290.54(-5.78)	33.1(-0.5)	0.780
5	Temperature, SSHA, EKE, Lun Illum, Hour, Long/Lat(TE)	298.64(2.31)	30.6(-3)	0.010
5	Temperature, CRT (RE), EKE, Lun Illum, Hour, Long/Lat(TE)	299.3(2.970)	29.2(-4.4)	0.014
5	Temperature, CRT (RE), SSHA, Lun Illum, Hour, Long/Lat(TE)	293.52(-2.81)	33.6(0)	0.176

Table 3: Change in Akaike Information Criterion (ΔAIC) and deviance explained (ΔDE) for environmental and spatial parameters in the final model.

Final Model	Variable	ΔAIC	ΔDE
AIC: 290.542	Hour of Sampling	19.02	6.3%
DE: 33.1%	Fraction of Lunar Illumination	17.91	7.7%
	Latitude, Longitude	13.65	9.7%
	Temperature at 5 m ($^{\circ}C$)	9.58	2.0%
	Sea Surface Height Anomaly (m)	8.10	1.9%
	Eddy Kinetic Energy ($m^2 s^{-2}$)	2.98	0.1%

FIGURE LEGENDS:

Figure 1: Schematic map of the Gulf of Mexico and Caribbean Sea showing the major ocean currents. Colors depict mean sea surface temperature estimates from the Hybrid Ocean Coordinate Model (HYCOM) 1/12° Reanalysis from April and May of 2010.

Figure 2: Distribution of sampling locations in the Gulf of Mexico and Caribbean in April-May a)2010 b)2011 and c)2012. Red symbols (+) indicate stations sampled and were used as model input. Black symbols (+) indicate stations sampled and were not used as model input due to sensor malfunctions and their shallow bathymetry (< 200 m depth). Red circles ● indicate stations that showed presence of swordfish larvae and were used as model input. Black circles ● indicate stations that showed presence of swordfish larvae and were not used as model input due to sensor malfunctions, lack of CTD casts, or their shallow bathymetry (< 200 m depth). Color scale indicative of sea surface temperature (SST).

Figure 3: Correlations between A) chlorophyll- *a* and temperature at 5 m ($r=-0.49$, $p<0.01$ and B) dissolved oxygen at 5 m and temperature at 5 m ($r=-0.74$, $p<0.01$).

Figure 4: Mean standard length of swordfish larvae by station caught in both neuston and S-10 nets from 2010-2012. Color scale indicative of sea surface temperature (SST).

Figure 5: The response curves for a) temperature at 5m (°C), b) sea surface height anomaly (m), c) eddy kinetic energy ($m^2 s^{-2}$), d) fraction of lunar illumination with the dark circle indicating the new moon and the open circle representing the full moon, and e) hour of sampling, with the open circle indicating local noon.

Figure 6: Catch of swordfish larvae in the Loop Current in 2012 overlaid on sea surface height anomaly (m). Red circles (●) indicate stations that showed presence of swordfish larvae.

1
2
3
4
5
6
7
8
9
10
11
12
13
14
15
16
17
18
19
20
21
22
23
24
25
26
27
28
29
30
31
32
33
34
35
36
37
38
39
40
41
42
43
44
45
46
47
48
49
50
51
52
53
54
55
56
57
58
59
60

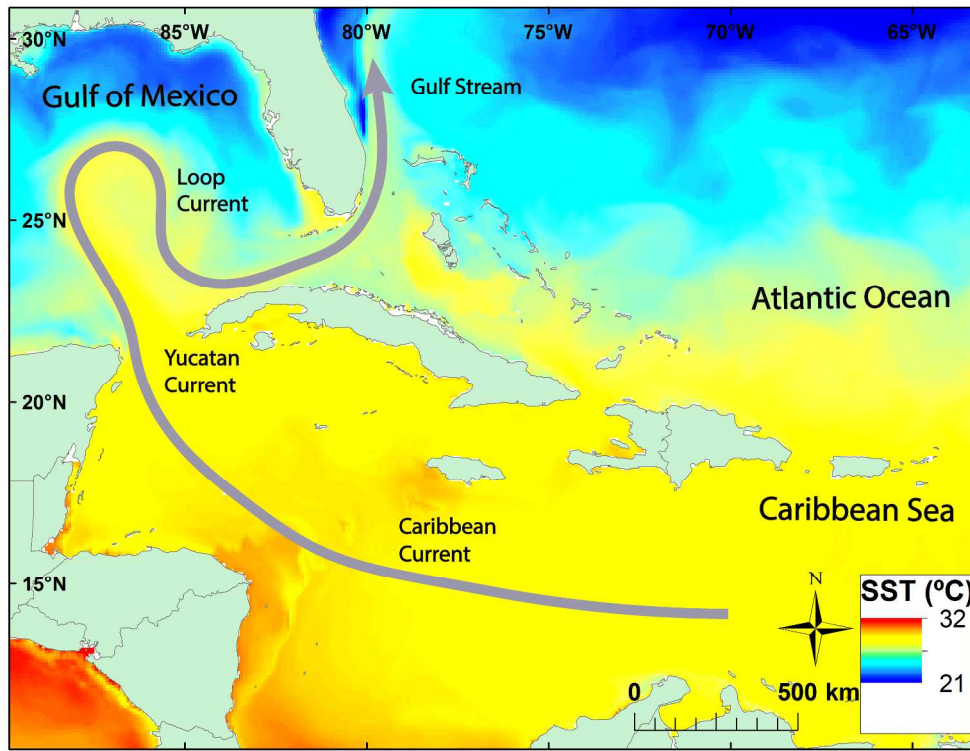


Figure 1: Schematic map of the Gulf of Mexico and Caribbean Sea showing the major ocean currents. Colors depict mean sea surface temperature estimates from the Hybrid Ocean Coordinate Model (HYCOM) 1/12o Reanalysis from April and May of 2010.

279x215mm (300 x 300 DPI)

view

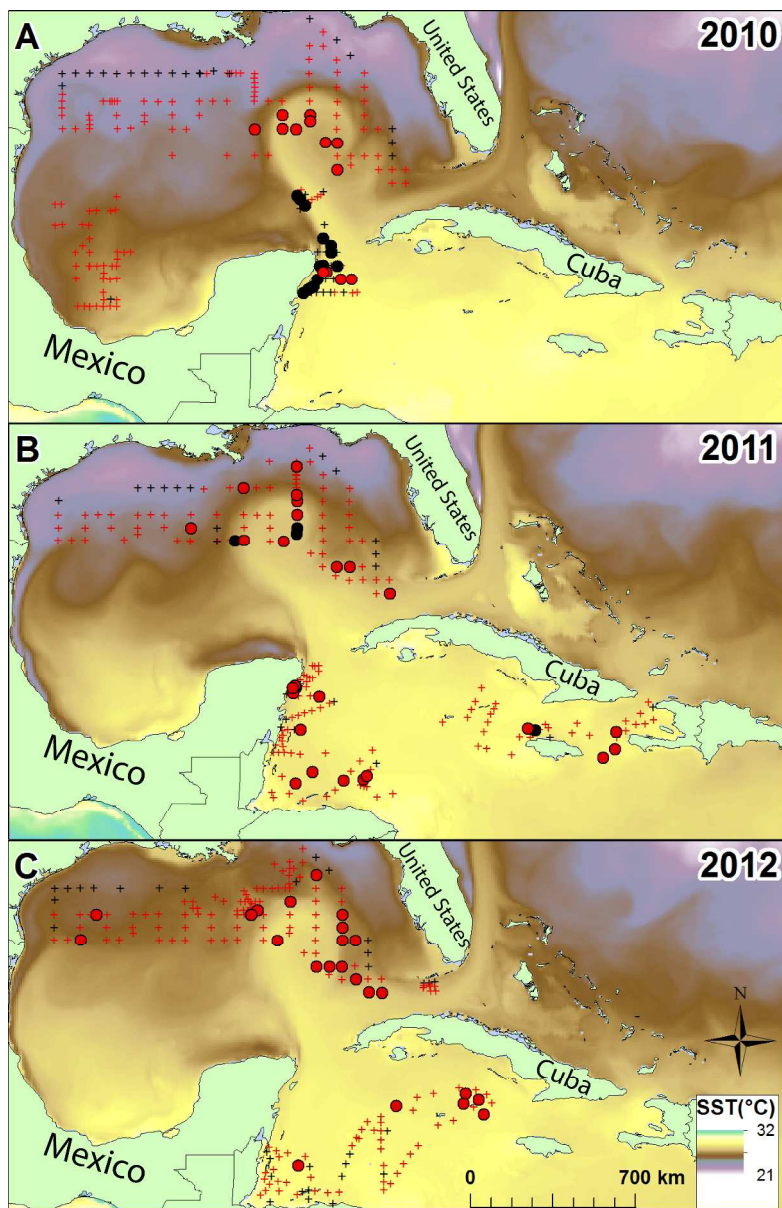


Figure 2: Distribution of sampling locations in the Gulf of Mexico and Caribbean in April-May a)2010 b)2011 and c)2012. Red symbols (+) indicate stations sampled and were used as model input. Black symbols (+) indicate stations sampled and were not used as model input due to sensor malfunctions and their shallow bathymetry (< 200 m depth). Red circles • indicate stations that showed presence of swordfish larvae and were used as model input. Black circles • indicate stations that showed presence of swordfish larvae and were not used as model input due to sensor malfunctions, lack of CTD casts, or their shallow bathymetry (< 200 m depth). Color scale indicative of sea surface temperature (SST).

279x431mm (300 x 300 DPI)

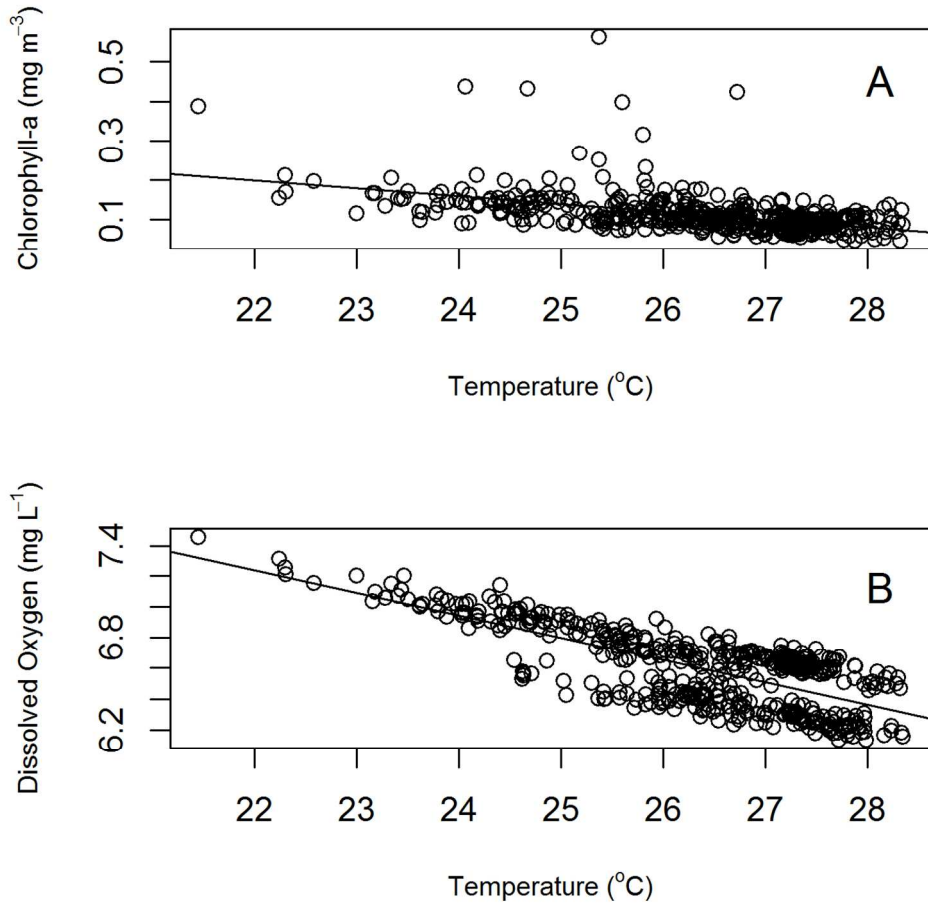


Figure 3: Correlations between A) chlorophyll- a and temperature at 5 m ($r=-0.49$, $p<0.01$) and B) dissolved oxygen at 5 m and temperature at 5 m ($r=-0.74$, $p<0.01$).

127x127mm (300 x 300 DPI)

1
2
3
4
5
6
7
8
9
10
11
12
13
14
15
16
17
18
19
20
21
22
23
24
25
26
27
28
29
30
31
32
33
34
35
36
37
38
39
40
41
42
43
44
45
46
47
48
49
50
51
52
53
54
55
56
57
58
59
60

1
2
3
4
5
6
7
8
9
10
11
12
13
14
15
16
17
18
19
20
21
22
23
24
25
26
27
28
29
30
31
32
33
34
35
36
37
38
39
40
41
42
43
44
45
46
47
48
49
50
51
52
53
54
55
56
57
58
59
60

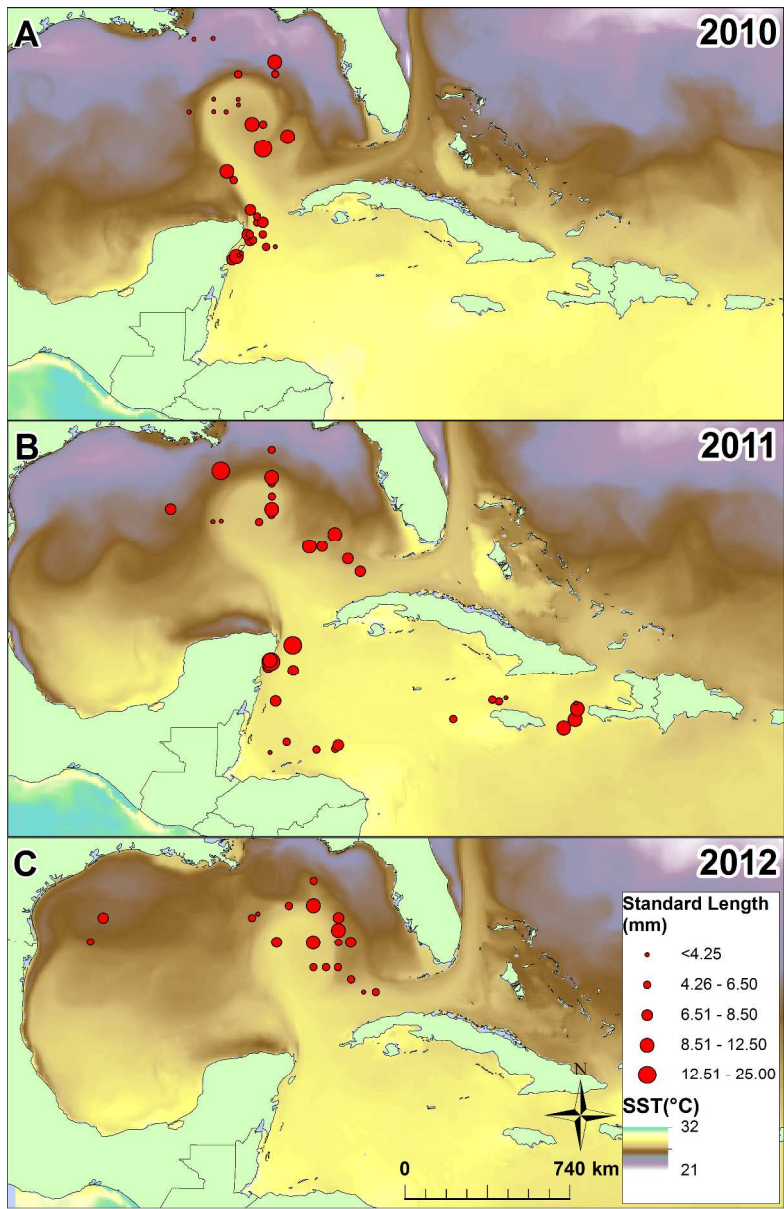


Figure 4: Mean standard length of swordfish larvae by station caught in both neuston and S-10 nets from 2010-2012. Color scale indicative of sea surface temperature (SST).

279x431mm (300 x 300 DPI)

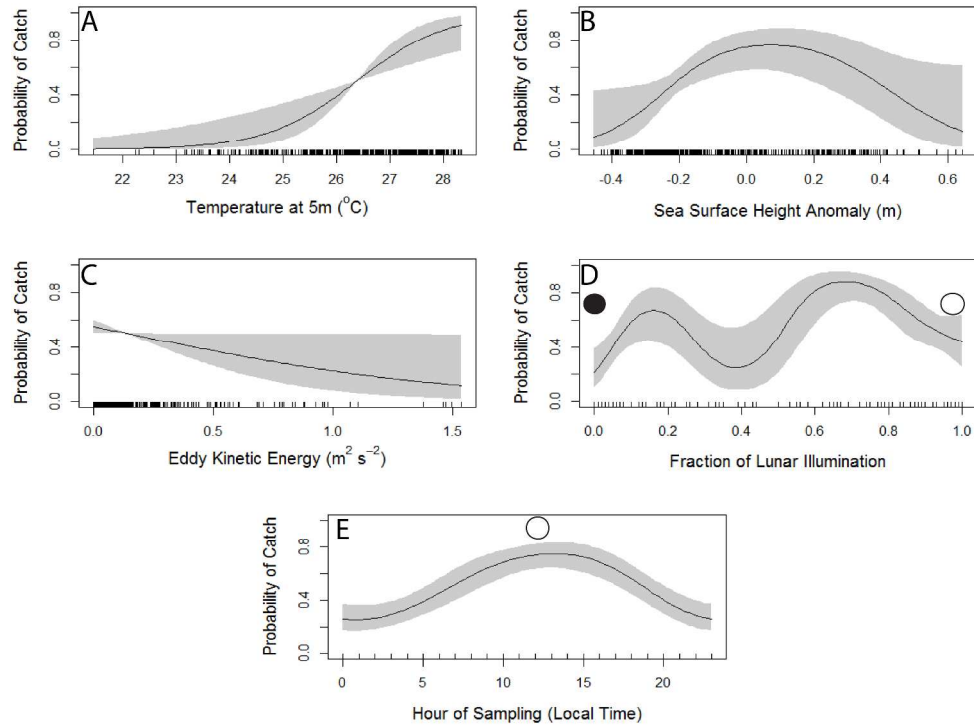


Figure 5: The response curves for a) temperature at 5m (oC), b) sea surface height anomaly (m), c) eddy kinetic energy (m² s⁻²), d) fraction of lunar illumination with the dark circle indicating the new moon and the open circle representing the full moon, and e) hour of sampling, with the open circle indicating local noon.

429x341mm (300 x 300 DPI)

ew

1
2
3
4
5
6
7
8
9
10
11
12
13
14
15
16
17
18
19
20
21
22
23
24
25
26
27
28
29
30
31
32
33
34
35
36
37
38
39
40
41
42
43
44
45
46
47
48
49
50
51
52
53
54
55
56
57
58
59
60

1
2
3
4
5
6
7
8
9
10
11
12
13
14
15
16
17
18
19
20
21
22
23
24
25
26
27
28
29
30
31
32
33
34
35
36
37
38
39
40
41
42
43
44
45
46
47
48
49
50
51
52
53
54
55
56
57
58
59
60

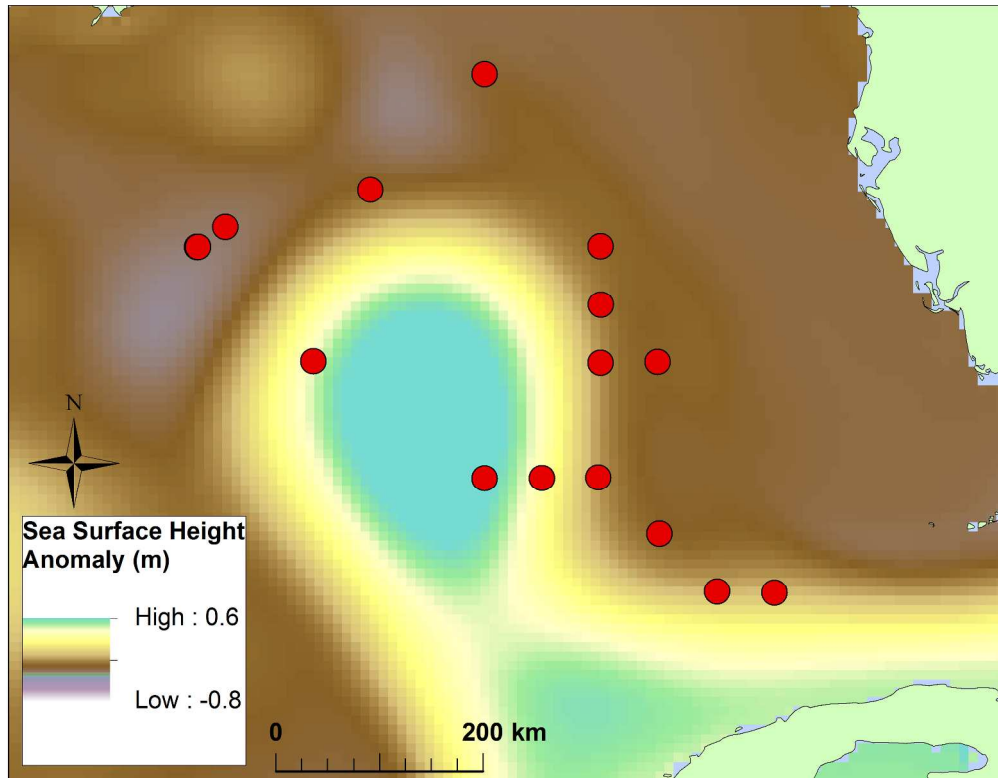


Figure 6: Catch of swordfish larvae in the Loop Current in 2012 overlaid on sea surface height anomaly (m). Red circles (●) indicate stations that showed presence of swordfish larvae.

279x215mm (300 x 300 DPI)

view

Supp. Table 1: Standard length, time, and location of swordfish larvae used in this study. N represents number of swordfish larvae caught by the S-10 and neuston net at each station.

Cruise	Date	Latitude	Longitude	Gear	N	Standard Length (mm)
GU1001	4/10/2010	20.7711	-86.5233	S-10	5	7.32-10.56
GU1001	4/10/2010	20.7773	-86.3936	S-10	2	4.73-6.78
GU1001	4/10/2010	20.9998	-86.6358	Neuston	1	6.66
GU1001	4/10/2010	21.0061	-86.004	S-10	3	3.54-6.31
GU1001	4/10/2010	21.0061	-86.004	Neuston	1	5.55
GU1001	4/10/2010	21.0071	-86.529	S-10	3	4-6.1
GU1001	4/11/2010	21.4841	-86.2376	S-10	1	6.01
GU1001	4/11/2010	21.4986	-85.9988	Neuston	1	8.07
GU1001	4/11/2010	21.7298	-86.2341	S-10	1	4.27
GU1001	4/11/2010	21.9985	-86.511	S-10	2	4.57-11.51
GU1001	4/12/2010	23.2012	-87.1788	S-10	1	4.3
GU1001	4/13/2010	23.4192	-87.3669	S-10	3	4.68-5.48
GU1001	4/13/2010	23.5531	-87.458	S-10	2	6.57-11.26
GU1001	4/28/2010	25.4893	-85.998	S-10	1	5.82
GU1001	4/28/2010	25.4926	-86.446	S-10	1	10.95
GU1001	4/29/2010	24.4922	-85.9979	S-10	2	3.72-25.68
GU1001	4/29/2010	24.9881	-84.9955	Neuston	1	10.05
GU1001	4/8/2010	19.994	-87.2475	S-10	3	4.77-11.28
GU1001	4/8/2010	20.0641	-87.1886	Neuston	17	2.86-6.72
GU1001	4/8/2010	20.1165	-87.0748	S-10	2	9.39-11.95
GU1001	4/8/2010	20.1693	-86.9623	S-10	5	3.55-4.4
GU1001	4/9/2010	20.2411	-86.8641	S-10	1	4.12
GU1001	4/9/2010	20.5005	-86.7161	S-10	2	3.81
GU1001	4/9/2010	20.5023	-85.8713	S-10	2	3.88-6.67
GU1001	4/9/2010	20.5105	-85.4938	S-10	2	3.64-3.89
GU1001	5/12/2010	26.0054	-87.5019	S-10	1	3.87
GU1001	5/12/2010	26.0148	-87.994	S-10	2	2.08-2.87
GU1001	5/12/2010	26.2829	-86.9944	S-10	2	2.8-3.12
GU1001	5/12/2010	26.501	-87.0005	S-10	3	3.78-4.32
GU1001	5/13/2010	26.5063	-87.9937	S-10	1	2.96
GU1001	5/22/2010	26.0029	-88.9991	S-10	1	4.11
GU1101	3/31/2011	18.8942	-78.2623	S-10	1	6.5
GU1101	4/1/2011	18.7633	-74.9499	S-10	1	3.9
GU1101	4/16/2011	16.975	-84.4886	S-10	3	4.2-5.1
GU1101	4/16/2011	17.118	-84.3708	S-10	1	6.9
GU1101	4/17/2011	16.9395	-85.2278	S-10	1	5.4
GU1101	4/19/2011	16.83	-87.0612	S-10	1	4
GU1101	4/19/2011	17.2533	-86.4111	S-10	1	6.46

	Cruise	Date	Latitude	Longitude	Gear	N	Standard Length (mm)
1							
2							
3							
4							
5	GU1101	4/19/2011	17.2533	-86.4111	Neuston	1	6.29
6	GU1101	4/21/2011	18.8438	-86.8526	S-10	2	5.6-8.9
7	GU1101	4/21/2011	18.8438	-86.8526	Neuston	1	7.6
8	GU1101	4/23/2011	20.0735	-86.1522	S-10	1	6.9
9	GU1101	4/23/2011	20.2111	-87.1356	S-10	1	7.9
10	GU1101	4/24/2011	21.0748	-86.1676	Neuston	1	13
11	GU1101	4/25/2011	20.4113	-87.1545	S-10	1	6.25
12	GU1101	4/25/2011	20.4113	-87.1545	Neuston	2	3.25-8
13	GU1101	4/25/2011	20.4343	-87.0401	S-10	1	17.5
14	GU1101	4/25/2011	20.4933	-87.0773	S-10	3	6.7-11.87
15	GU1101	4/3/2011	17.7941	-75.4387	S-10	1	10
16	GU1101	4/3/2011	18.1151	-74.99	S-10	1	9.5
17	GU1101	4/3/2011	18.5355	-74.9028	Neuston	1	10.7
18	GU1101	4/3/2011	18.5355	-74.9028	Neuston	1	10.7
19	GU1101	4/3/2011	18.5355	-74.9028	Neuston	1	10.7
20	GU1101	4/5/2011	18.8322	-78.0036	S-10	1	4.8
21	GU1101	4/5/2011	18.8322	-78.0036	S-10	1	4.8
22	GU1101	4/5/2011	18.8322	-78.0036	S-10	1	4.8
23	GU1101	4/5/2011	18.9693	-77.7284	Neuston	1	3.4
24	GU1101	4/6/2011	18.1357	-79.8196	Neuston	1	6.2
25	GU1101	5/15/2011	28.009	-89.0103	S-10	1	23.1
26	GU1101	5/22/2011	26.5008	-90.999	S-10	1	8.37
27	GU1101	5/23/2011	25.9993	-89.3346	S-10	1	3.79
28	GU1101	5/23/2011	25.9993	-89.3346	S-10	1	3.79
29	GU1101	5/24/2011	26.0165	-88.9946	S-10	1	3.84
30	GU1101	5/25/2011	25.9875	-87.498	S-10	3	4.95-8.82
31	GU1101	5/25/2011	25.9875	-87.498	S-10	3	4.95-8.82
32	GU1101	5/25/2011	26.2705	-87.0073	S-10	12	3.25-6.99
33	GU1101	5/25/2011	26.489	-86.9971	S-10	3	6.76-11.86
34	GU1101	5/25/2011	26.489	-86.9971	Neuston	1	5.32
35	GU1101	5/26/2011	26.9955	-86.992	S-10	12	3.44-9.32
36	GU1101	5/26/2011	26.9955	-86.992	S-10	12	3.44-9.32
37	GU1101	5/26/2011	26.9955	-86.992	Neuston	7	6.73-13.94
38	GU1101	5/26/2011	27.7516	-87.0018	S-10	1	9.42
39	GU1101	5/27/2011	28.826	-87.0031	S-10	1	6.02
40	GU1101	5/3/2011	23.9987	-83.4882	S-10	2	4.85-10.71
41	GU1101	5/3/2011	23.9987	-83.4882	S-10	2	4.85-10.71
42	GU1101	5/4/2011	24.5111	-83.986	Neuston	1	8.09
43	GU1101	5/5/2011	24.9918	-85.5051	S-10	1	8.7
44	GU1101	5/5/2011	24.9918	-85.5051	S-10	1	8.7
45	GU1101	5/5/2011	24.9925	-85.0026	S-10	3	6.04-13.02
46	GU1101	5/8/2011	27.5095	-86.994	S-10	1	4.88
47	GU1201	4/30/2012	24.986	-85.5063	S-10	8	4.37-9.8
48	GU1201	4/30/2012	24.9925	-85.0145	S-10	1	4.74
49	GU1201	5/1/2012	24.0006	-83.9836	S-10	1	4.07
50	GU1201	5/1/2012	24.5016	-84.4856	S-10	1	5.82
51	GU1201	5/1/2012	24.5016	-84.4856	S-10	1	5.82
52	GU1201	5/17/2012	26.9988	-88.4993	S-10	2	2.79-3.64
53	GU1201	5/2/2012	23.9906	-83.4855	S-10	1	6.09
54	GU1201	5/2/2012	23.9906	-83.4855	S-10	1	6.09
55	GU1201	5/22/2012	26.0206	-95.0118	S-10	1	4.87
56	GU1201	5/22/2012	26.0206	-95.0118	Neuston	1	4.19
57	GU1201	5/22/2012	26.0206	-95.0118	Neuston	1	4.19
58	GU1201	5/26/2012	26.9991	-88.4921	S-10	1	4.76
59							
60							

Cruise	Date	Latitude	Longitude	Gear	N	Standard Length (mm)
GU1201	5/26/2012	27.1701	-88.254	S-10	2	3.62-3.93
GU1201	5/3/2012	25.9948	-84.9971	S-10	2	4.54-7.96
GU1201	5/3/2012	26.0026	-84.5	S-10	1	8.05
GU1201	5/3/2012	26.4983	-84.9938	S-10	1	16.52
GU1201	5/3/2012	26.4983	-84.9938	Neuston	1	5.15
GU1201	5/3/2012	27.0031	-84.9968	S-10	2	7.12-7.73
GU1201	5/3/2012	27.0031	-84.9968	Neuston	1	9.59
GU1201	5/5/2012	27.506	-86.005	Neuston	1	11.44
GU1201	5/5/2012	28.5051	-86.0021	S-10	1	4.55
GU1201	5/6/2012	24.9853	-86.0033	S-10	5	3.22-5.07
GU1201	5/6/2012	24.9853	-86.0033	Neuston	1	8.9
GU1201	5/6/2012	26.0016	-86.0136	Neuston	1	12.47
GU1201	5/7/2012	26.0066	-87.4911	S-10	1	8.37
GU1201	5/9/2012	27.4965	-86.9958	S-10	1	7.69
GU1201	5/9/2012	27.4965	-86.9958	Neuston	3	5.03-6.79

Peer Review